Biochimica et Biophysica Acta 1818 (2012) 2623–2635

Contents lists available at SciVerse ScienceDirect

Biochimica et Biophysica Acta

journal homepage: www.elsevier.com/locate/bbamem

Synergistic action of *Galleria mellonella* anionic peptide 2 and lysozyme against Gram-negative bacteria

Agnieszka Zdybicka-Barabas [a], Pawel Mak [b], Anna Klys [b,1], Krzysztof Skrzypiec [c], Ewaryst Mendyk [c], Marta J. Fiołka [a], Małgorzata Cytryńska [a,*]

[a] Department of Immunobiology, Institute of Biology and Biochemistry, Maria Curie-Skłodowska University, Akademicka 19 St., 20–033 Lublin, Poland
[b] Department of Analytical Biochemistry, Faculty of Biochemistry, Biophysics and Biotechnology, Jagiellonian University, Gronostajowa 7 St., 30–387 Krakow, Poland
[c] Analytical Laboratory, Faculty of Chemistry, Maria Curie-Skłodowska University, M.C. Skłodowska Square 5, 20–031 Lublin, Poland

ARTICLE INFO

Article history:
Received 27 February 2012
Received in revised form 15 May 2012
Accepted 6 June 2012
Available online 14 June 2012

Keywords:
Defense peptide
Lysozyme
Anionic peptide 2
Galleria mellonella
Atomic force microscopy

ABSTRACT

Lysozyme and antimicrobial peptides are key factors of the humoral immune response in insects. In the present work lysozyme and anionic defense peptide (GMAP2) were isolated from the hemolymph of the greater wax moth *Galleria mellonella* and their antibacterial activity was investigated. Adsorption of *G. mellonella* lysozyme on the cell surface of Gram-positive and Gram-negative bacteria was demonstrated using immunoblotting with anti-*G. mellonella* lysozyme antibodies. Lysozyme effectively inhibited the growth of selected Gram-positive bacteria, which was accompanied by serious alterations of the cell surface, as revealed by atomic force microscopy (AFM) imaging. *G. mellonella* lysozyme used in concentrations found in the hemolymph of naive and immunized larvae, perforated also the *Escherichia coli* cell membrane and the level of such perforation was considerably increased by GMAP2. GMAP2 used alone did not perforate *E. coli* cells nor influence lysozyme muramidase activity. However, the peptide induced a decrease in the turgor pressure of the bacterial cell. Moreover, in the samples of bacteria treated with a mixture of lysozyme and GMAP2 the sodium chloride crystals were found, suggesting disturbance of ion transport across the membrane leading to cell disruption. These results clearly indicated the synergistic action of *G. mellonella* lysozyme and anionic peptide 2 against Gram-negative bacteria. The reported results suggested that, thanks to immune factors constitutively present in hemolymph, *G. mellonella* larvae are to some extent protected against infection caused by Gram-negative bacteria.

1. Introduction

Antimicrobial or defense peptides are key factors of the innate immune response against invading pathogens in animals. Most antimicrobial peptides are small, amphipathic, cationic molecules. According to their amino acid sequence and secondary structure, they are usually classified into three classes: (i) alpha-helical linear peptides without cysteine residues, *e.g.* cecropins, (ii) peptides stabilized by disulfide bridges, *e.g.* defensins, and (iii) peptides with overrepresentation of certain single amino acid, as *e.g.* proline-rich peptides. In majority of antimicrobial peptides the relatively high content of positively charged arginine and lysine residues facilitates interaction with anionic surface of pathogen cells. The interaction with membrane phospholipids is possible thanks to the presence of both hydrophobic as well as hydrophilic domains in the antimicrobial peptide molecules. Several modes of interaction with microbial membranes have been proposed for cationic defense peptides: (i) carpet-like model, (ii) barrel-stave model, (iii) toroidal pore model, and (iv) aggregate formation model. Binding of the cationic peptides to the phospholipid molecules present in a microbial membrane can induce formation of transmembrane pores of different structures, changes in permeability, and even disruption of the membrane. Besides cell membrane phospholipids, outer surface lipids and outer membrane as well as integral membrane proteins can be the major targets for antimicrobial peptides. Some peptides can also traverse across the cell membrane, penetrate the pathogen cell and, after binding to DNA, RNA or heat shock proteins, they can disturb the proper functioning of the cell [1–10].

Among antimicrobial peptides the examples of anionic molecules have also been described. Defense peptides with such negative net charge were first isolated from ovine pulmonary surfactant and named surfactant-associated anionic peptides (AP). They are small molecules (molecular weight 720–825 Da) containing homopolymeric regions of 5 to 7 aspartic acid residues. The peptides require zinc ions for maximum antimicrobial activity, however, to date, the mechanism of their bactericidal action is not known. One can speculate that the anionic peptides

* Corresponding author. Tel.: +48 81 537 50 50; fax: +48 81 537 59 01.
E-mail address: cytryna@poczta.umcs.lublin.pl (Mł. Cytryńska).
[1] Present address: Biocentrum Ltd., Bobrzynskiego 14, 30–348 Krakow, Poland.

0005-2736/$ – see front matter © 2012 Elsevier B.V. All rights reserved.
doi:10.1016/j.bbamem.2012.06.008

may inhibit the ribonuclease activity in the ribosomes or induce flocculation of the cell content [11–13]. Examples of anionic defense peptides have also been characterized in invertebrates. From the hard tick *Amblyomma hebraeum*, a defensin-like peptide of pI 4.44 exhibiting activity against *Escherichia coli* and *Staphylococcus aureus* was isolated [14]. Similarly, an anionic defensin-like peptide with predicted pI 4.12 was described in the lepidopteran insect, *Bombyx mori* [15]. Two anionic defense peptides, named anionic peptides 1 and 2 (GMAP1 and GMAP2), were discovered among the defense peptides found in the hemolymph of the greater wax moth *Galleria mellonella*. GMAP2 is 60 amino acids long, 6.98 kDa peptide of pI 4.79. The sequence of this peptide contains 8 residues of glutamic acid, 3 residues of aspartic acid and does not contain cysteine, histidine, arginine nor tryptophan. The amino acid sequence of GMAP2 is unique and to date, no significantly similar sequences of other peptides nor proteins have been found. Interestingly, GMAP2 is present constitutively in hemolymph of non-immunized *G. mellonella* larvae in a relatively high concentration estimated as 11.7 μM (±3.17). The peptide is moderately active against selected Gram-positive bacteria and yeasts *in vitro* [16,17].

Another important component of the insect humoral immune response is lysozyme. Lysozymes have been isolated and studied from many insect species, including representatives of Lepidoptera, Diptera, Coleoptera as well as Hymenoptera [18–30]. According to their amino acid sequence and other physico-chemical properties, most of the insect lysozymes belong to c-type family of lysozymes [31].

The lysozyme of the lepidopteran *G. mellonella* which contains 121 amino acids, has a predicted molecular weight 14027 Da and isoelectric point pI = 9.28 (SWISS-PROT data bank: locus LYC_GALME, accession P82174). The antibacterial and antifungal activity of *G. mellonella* lysozyme was described earlier [26,32]. It was demonstrated that, similarly to some other lepidopteran lysozymes, *G. mellonella* lysozyme exhibited a low activity against selected Gram-negative bacteria (*E. coli* K112, *E. coli* DH5α, *Salmonella paratyphi* A, *S. choleraesuis*) [26], in addition to its high anti-Gram-positive bacteria activity. Lysozyme in *G. mellonella* is synthesized constitutively and is present in the hemolymph of naive larvae in the concentration of 0.76 μM (±0.17) [17]. Based on the experiments performed using egg white lysozyme (EWL), it was suggested that lysozyme could act synergistically with certain *G. mellonella* antimicrobial peptides and proteins against Gram-negative bacteria [33]. It was also demonstrated that EWL activity against *M. luteus* increased in the presence of apolipophorin III [34], whereas *E. coli* became more sensitive to attacins, cecropins and insect defensins in the presence of lysozyme [35,36].

The constitutive presence of high GMAP2 concentrations in *G. mellonella* hemolymph together with its relatively low antimicrobial activity prompted us to investigate the effects of this defense peptide on the antibacterial activity of *G. mellonella* lysozyme. X-ray analysis, imaging by atomic force microscopy (AFM) and scanning electron microscopy (SEM) were used to characterize the alterations caused by the compounds studied in the bacteria cell surface and morphology. Moreover, AFM was used to determine the influence of *G. mellonella* lysozyme and GMAP2 on nanomechanical properties of the bacterial cells, such as elasticity and adhesive forces.

2. Materials and methods

2.1. Bacterial strains and culture conditions

Gram-positive bacteria (*Bacillus circulans* ATCC 61, *Corynebacterium avis*, *Listeria monocytogenes*, *Micrococcus luteus* ATCC 10240, *Rhodococcus aqui*, *Sarcina lutea*, *S. aureus* ATCC 25922) were grown at 28 °C, whereas Gram-negative bacteria (*E. coli* D31, *E. coli* JM83, *Klebsiella pneumoniae*, *Pseudomonas aeruginosa* H3, *Salmonella typhimurium* LT2, *Sinorhizobium meliloti*) were cultured at 37 °C (with exception of *S. meliloti* which was grown at 28 °C) in 2.5% Luria–Bertani (LB) medium. Bacteria in the logarithmic phase of growth were used during the experiments.

2.2. Insect immune challenge, hemolymph collection, and preparation of methanolic extracts

Larvae of the greater wax moth *G. mellonella* (Lepidoptera: Pyralidae) were reared on a natural diet — honeybee nest debris at 30 °C in the dark. Last instar larvae (250–300 mg in weight) were used throughout the study.

For the immune challenge, the larvae were pierced with a needle dipped into a pellet containing live cells of *E. coli* D31 and *M. luteus* and the hemolymph was collected 24 h after the immunization. The hemolymph was collected into sterile and chilled Eppendorf tubes containing a few crystals of phenylthiourea (PTU) to prevent melanization, as described earlier [37]. The hemocyte-free hemolymph was obtained by centrifugation at 200×*g* for 5 min to pellet the hemocytes and the supernatant was subsequently centrifuged at 20,000×*g* for additional 15 min at 4 °C to pellet the cell debris. The cell-free hemolymph was stored at −20 °C until needed. Methanolic extracts containing antimicrobial peptides and proteins below 30 kDa were prepared from the cell-free hemolymph as described earlier [16].

2.3. Purification of *G. mellonella* lysozyme and anionic defense peptide

G. mellonella lysozyme and AP2 were purified from the immune hemolymph extract using a modified technique described in our previous study [16]. Briefly, the hemolymph extract, deprived of lipids and freeze-dried, was dissolved in 0.1% trifluoroacetic acid (TFA) and subjected to the HPLC chromatography using a Supelcosil LC-18-DB 4.6 mm×250 mm column (Sigma-Aldrich-Fluka-Supelco Company, St. Louis, MO, USA), two buffer set, A: 0.1% TFA (v/v), B: 0.07% TFA, 80% acetonitrile (v/v), a linear gradient from 36 to 68% of buffer B over 30 min and 1 ml/min flow rate. The collected fractions were freeze-dried, redissolved in water, subjected to SDS-PAGE electrophoresis [38], electroblotted onto a polyvinylidene difluoride (PVDF) membrane, stained with Coomassie Brillant Blue R-250 and then identified by N-terminal amino acid sequencing on Procise 491 (Applied Biosystems, Foster City, CA, USA). The results of the electrophoresis and sequencing proved that anionic peptide 2 was obtained in a pure form. On the other hand, the slightly contaminated fraction containing lysozyme was additionally purified by gel filtration chromatography on a Superdex Peptide 10/300 GL column (Pharmacia Biotech, Uppsala, Sweden), using 0.1% TFA supplemented with 40% (v/v) acetonitrile as mobile phase and 0.4 ml/min flow rate. The purified proteins and peptides were lyophilized and stored at −80 °C. For the experiments, they were redissolved in sterile deionized water.

2.4. Adsorption of lysozyme on the bacterial cell surface

Adsorption of *G. mellonella* lysozyme on bacterial cells was performed as described in our previous paper [39]. In brief, the suspensions of bacteria (200 μl, OD_{600} = 1.0) growing overnight in a liquid LB medium were centrifuged at 1600×*g* at 4 °C for 10 min. Obtained bacterial pellet was suspended in 20 μl of a mixture of 0.9% NaCl and 20% acetic acid (1:1, v/v). After 5-min incubation at room temperature, 100 μl of 1 M Tris–HCl pH 8.2 was added to neutralize the acidic pH. After centrifugation, the pellet was suspended in 20 μl of 10 mM Tris–HCl pH 8.2. The bacterial suspension was incubated without and in the presence of hemolymph extracts (5 μg of total protein) for 5 min at 30 °C and centrifuged. The pellet containing proteins adsorbed on the bacterial cells was washed twice in 50 μl of sterile water and suspended in 20 μl of 0.5 M ammonium formate pH 6.4. Laemmli sample buffer was added to the pellet and to the obtained supernatant containing proteins that did not adsorb on the bacterial surface. The samples were subjected to Tris-glycine SDS-PAGE [40] and subsequent immunoblotting with antibodies against *G. mellonella* lysozyme.

2.5. Immunoblotting

The samples subjected to 13.8% Tris-glycine SDS-PAGE were electroblotted onto PVDF membranes (Millipore) for 90 min at 350 mA, rinsed in TBS (10 mM Tris–HCl pH 7.4, 0.9% NaCl) and blocked in 3% skim milk in TBS For lysozyme identification, the membranes were then probed with rabbit polyclonal antibodies (1:1000) to *G. mellonella* lysozyme (a generous gift from Prof. I.H. Lee, Department of Life Science, Hoseo University, South Korea). Alkaline phosphatase-conjugated goat anti-rabbit IgG (1:30,000) was used as second antibody and the immunoreactive bands were visualized by incubation with *p*-nitro blue tetrazolium chloride and 5-bromo-4-chloro-3-indolyl phosphate (BCIP/NBT).

2.6. Antibacterial activity of G. mellonella lysozyme

2.6.1. Measurement of the optical density of the live bacteria suspension

Ten microliters of suspension of live log-phase bacterial cells in LB medium ($OD_{600} = 0.2$) was incubated without (control) or in the presence of *G. mellonella* lysozyme (final concentration 0.015 μM) for 1.5 h at 28 °C. After incubation, the optical density of the bacterial suspensions was determined at 600 nm.

2.6.2. Bacterial membrane permeabilization assay

The ability of the compounds studied to perforate the Gram-negative bacteria membrane was determined using the *E. coli* JM83 strain bearing plasmid pCH110 (Pharmacia-Amersham, Piscatway, NJ, USA) encoding constitutively synthesized cytoplasmic β-galactosidase and ampicilin resistance [41]. *G. mellonella* lysozyme, GMAP2, and mixtures of both compounds in 20 mM phosphate buffer pH 6.8 (23 μl) were preincubated for 15 min at 37 °C in Eppendorf tubes. Then, 2 μl of live mid-logarithmic phase cells suspension (5×10^5 CFU) in the same buffer was added and the samples were incubated for 45 min at 37 °C (the final concentrations of lysozyme — 0.5 μM and 5.0 μM; AP2 — 0.5 μM and 5.0 μM). Next, 220 μl of 20 mM HEPES/150 mM NaCl buffer pH 7.5 and 5 μl of the β-galactosidase colorimetric substrate (50 mM aqueous solution of *p*-nitrophenyl-β-D-galactopyranoside) were added. The samples were transferred into the wells of a flat-bottom polyethylene 96-well plate and vortexed; after 90 min of incubation at 37 °C absorbance, proportional to the amount of released β-galactosidase, were measured at 405 nm. Two types of the control samples were prepared: (i) live bacteria and (ii) dead bacteria (after lysis using EWL 3 mg/ml and 0.1% Triton X-100) incubated without peptide addition. The perforation level of the dead bacteria was assumed as 100%. All assays were performed in triplicate.

2.7. AFM and SEM imaging of bacterial cells

2.7.1. Preparation of bacterial samples

One hundred microliters of suspension containing log-phase bacterial cells ($OD_{600} = 0.2$) cultured in the LB medium was centrifuged at 8000 ×*g* for 10 min at 4 °C. The cells were gently washed with 100 μl of sterile 20 mM phosphate buffer pH 6.8 and centrifuged as described. Then, the bacteria were incubated for 1.5 h without (control) and in the presence of purified *G. mellonella* lysozyme (final concentration 0.015 μM for the Gram-positive bacteria; 1.0 μM and 5.0 μM for the Gram-negative bacteria) at 28 °C in 20 mM phosphate buffer pH 6.8 in a final volume of 130 μl (in triplicate). *E. coli* JM83 and *K. pneumoniae* were also treated with GMAP2 (the final concentrations 1.0 μM and 5.0 μM) and with a mixture of lysozyme and GMAP2 (lysozyme and GMAP2 molar ratio 1:1). For determination of a neutral protein effect, the bacteria were incubated with bovine serum albumin (BSA, Sigma; dissolved in sterile deionised water) under the same conditions. After incubation, the bacterial suspensions were centrifuged as described above. The bacterial pellets were gently washed once with 150 μl of sterile 20 mM phosphate buffer pH 6.8 and then twice with 100 μl of apyrogenic water. After final centrifugation, the bacteria were suspended in 5 μl of apyrogenic water. For AFM, the samples were then applied on the surface of freshly cleaved mica discs and allowed to dry overnight at 28 °C before imaging.

For SEM, the samples were fixed with 4% glutaraldehyde in 0.1 M phosphate buffer pH 7.0. Then, the cells were stained with 1.5% osmium tetroxide in the same buffer for 30 min at room temperature. Afterwards, the cells were dehydrated stepwise in a graded series of acetone, allowed to dry overnight and sputter-coated with gold. Some probes were prepared for SEM after being examined by AFM. For this purpose, the dry samples on mica discs were sputtered with an ultra thin gold-palladium film.

2.7.2. AFM imaging

The alterations in the bacterial cell surface caused by *G. mellonella* lysozyme and GMAP2 were imaged by AFM (Analytical Laboratory, Faculty of Chemistry, UMCS, Lublin, Poland). All measurements in the contact and tapping operation modes were carried out using a NanoScope V AFM (Veeco, USA) equipped with NanoScope 8.10 software and a piezoscanner of a maximum scan range of 150 μm × 150 μm. For the contact mode a silicon nitride tip with a spring constant of 0.06 N/m, whereas for the tapping mode a rectangular Si cantilever/tip (Veeco, USA) with a spring constant of 20–80 N/m and resonance frequency of 300 kHz were used. The resolution of the scans obtained was 256 × 256 pixels. The topography and amplitude/deflection images were obtained simultaneously. Three fields on each mica disc were imaged. The data were analyzed with WSxM 5.0 software (Nanotec, Spain). The roughness values were measured over the entire bacterial cell surface on 600 × 600 nm areas. The average surface root-mean-square (RMS) roughness of the cells was calculated from ten fields estimated during two independent experiments.

For estimation of *G. mellonella* lysozyme and GMAP2 influence on bacterial cells elasticity and adhesion properties, Young's modulus and adhesion to the AFM tip were determined, respectively. The force measurements were performed in "PeakForce QNM" operation mode using a silicon tip on nitride lever, SCANASYST-AIR, with a spring constant of 0.4 N/m (Veeco, USA). The data were analyzed with Nanoscope Analysis ver. 1.40 software (VEECO, USA).

2.7.3. SEM imaging

The alterations caused by *G. mellonella* lysozyme and GMAP2 (the final concentrations 1.0 μM) on the cell surface of the Gram-negative bacteria tested were also imaged by scanning electron microscopy. The samples were examined under a VEGA 3 LMU microscope (Tescan, Czech Republic) (Institute of Biology and Biochemistry, Faculty of Biology and Biotechnology, UMCS, Lublin, Poland).

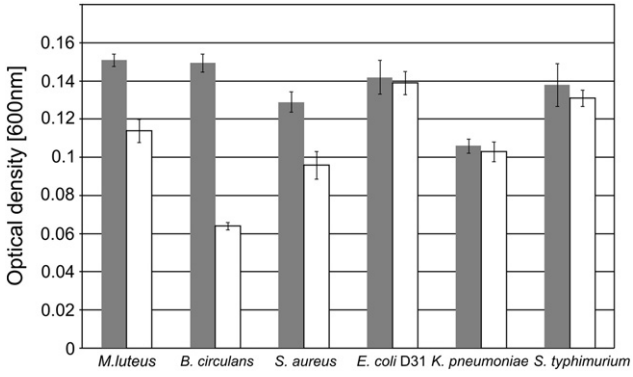

Fig. 1. Growth inhibition of bacteria by *G. mellonella* lysozyme. The bacteria were incubated without (control) or in the presence of lysozyme (0.015 μM) for 1.5 h. Then the optical density of the bacterial suspensions was determined at 600 nm. The diagram presents results ± SD of three independent experiments each performed in triplicate.

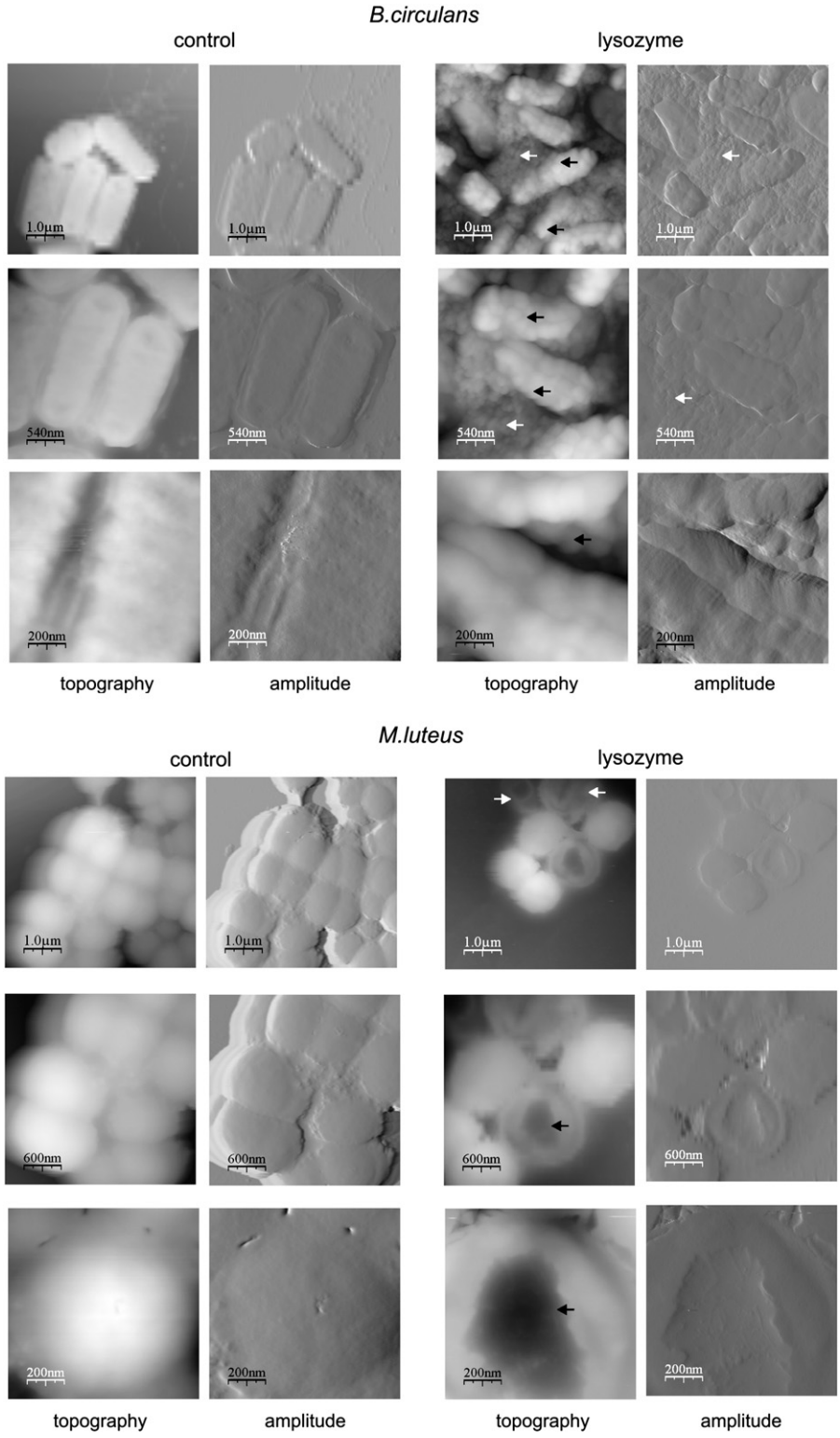

Fig. 2. The effect of *G. mellonella* lysozyme on *Bacillus circulans* and *Micrococcus luteus* cells. The bacteria were incubated without (control) or in the presence of lysozyme (0.015 μM) for 1.5 h and then imaged using AFM. Topography and amplitude images of the bacterial cells are presented. The black and white arrows in the *B. circulans* images indicate the granular structures appearing on the surface of the lysozyme-treated cells and the amorphous material present around the cells, respectively. The black and white arrows in the *M. luteus* images indicate deep concavities appearing on the surface of the lysozyme-treated cells and the "cell ghosts", respectively.

Some investigations of bacteria in the samples previously examined by AFM were performed using a FEI Quanta 3D FED scanning electron microscope equipped with an EDS detector (Analytical Laboratory, Faculty of Chemistry, UMCS, Lublin, Poland). The bacteria on mica foil were sputtered with an ultra thin gold-palladium film. The pictures of the bacterial topography were taken under high vacuum conditions at 30 kV accelerating voltage. An ETD (SE) detector was used to collect the signals from the scattered electrons.

2.8. X-ray analysis

The elemental analysis of randomly selected points on the observed by AFM rectangular structures as well as the images on the bacterial surface (control) was performed under FEI Quanta 3D FEG scanning electron microscope (Analytical Laboratory, Faculty of Chemistry, UMCS, Lublin, Poland). An imaging under SEM was performed after sputtering the samples with a thin gold-palladium film. Energy dispersive X-ray (EDX) microanalysis was made using a silicon drift detector (SDD) operating at 30 kV acceleration voltage. The microanalysis was carried out without any shadowing and the concentrations of the elements were determined using the standardless method. A composition of the elements in the rectangular structures was calculated on the basis of the differential analysis of spectra obtained for the structures and the control areas.

2.9. Interaction between molecules of G. mellonella lysozyme and GMAP2

To elucidate the formation of an eventual intermolecular complex the solutions of lysozyme and GM anionic peptide 2 in 50 mM sodium phosphate pH 7.4, 0.15 M NaCl were mixed together at 1:1 or 1:5 molar proportions. After incubation for 1 h at room temperature both mixtures were then analyzed by size exclusion chromatography on Superdex Peptide 10/300 GL column (GE Healthcare, USA) equilibrated in 0.1 M sodium phosphate pH 7.4 at 0.4 ml/min flow rate.

2.10. Other methods

The protein concentration was estimated by the Bradford method using BSA as a standard [42]. Polyacrylamide gel electrophoresis of proteins was performed by 13.8% Tris-glycine SDS-PAGE according to Laemmli [40]. The peptides were resolved by 16.5% Tris-tricine SDS-PAGE according to Schägger and von Jagow [38]. The data are presented as means ± standard deviation (SD) for at least three experiments. In order to compare two means, statistical analysis was performed by Student's *t*-test.

3. Results

3.1. Antibacterial activity of G. mellonella lysozyme

The activity of purified *G. mellonella* lysozyme was tested against selected Gram-positive (*B. circulans*, *M. luteus*, and *S. aureus*) and Gram-negative (*E. coli*, *K. pneumoniae*, and *S. typhimurium*) bacteria. After 1.5 h incubation, lysozyme in a concentration of 0.015 μM inhibited growth of all Gram-positive bacteria. *B. circulans* was the most sensitive to lysozyme action (growth inhibition in about 60%). In contrast, the Gram-negative bacteria tested under the same conditions were not sensitive to *G. mellonella* lysozyme (Fig. 1).

The decrease in the optical density of the Gram-positive bacteria cultures caused by 0.015 μM *G. mellonella* lysozyme was accompanied by evident alterations in the bacterial cell surface. The alterations in the *B. circulans* and *M. luteus* cell surfaces were imaged using atomic force microscopy. *B. circulans* control cells were smooth surfaced and rod-shaped (Figs. 2, 3). After exposure to *G. mellonella* lysozyme, the cell surface became highly granular with irregular grooves (50 nm depth; diameter about 200 nm). Cells that were still rod-shaped were surrounded by an amorphous material, probably the remains of the dead cells. *M. luteus* control cells were regularly round and had a smooth cell surface (Figs. 2,

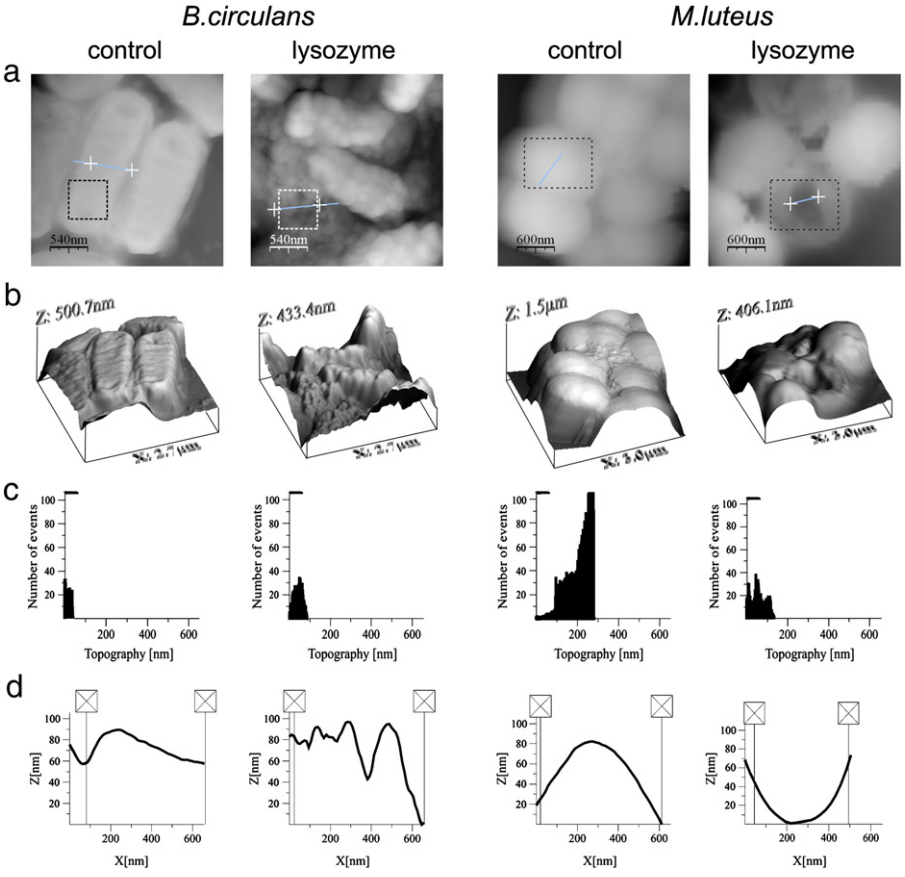

Fig. 3. Analysis of the alterations in *B. circulans* and *M. luteus* cell surfaces after incubation with *G. mellonella* lysozyme. The bacteria were incubated without (control) or in the presence of lysozyme (0.015 μM) for 1.5 h and then imaged using AFM. An analysis of contact mode images of the whole cells is presented. (a) topography and (b) 3D images; (c) roughness analysis of the square area marked in (a); (d) section profiles corresponding to black/white lines in (a).

3). In contrast, many lysozyme-treated *M. luteus* cells were damaged and they exhibited deep concavities (70 nm depth, diameter about 500 nm) formed usually in the central part of the cell. "Cell ghosts" were also noticed. The cell surface alterations detected were confirmed by analysis of cell surface roughness. The roughness root-mean-square (RMS) values for control *B. circulans* and *M. luteus* were estimated as 24.46 (±10.62) and 44.48 (±16.52), respectively. In contrast, RMS roughness values for lysozyme-treated *B. circulans* and *M. luteus* were calculated as 38.88 (±17.00; $p = 0.004$) and 35.07 (±9.37; $p = 0.045$), respectively.

3.2. Adsorption of G. mellonella lysozyme to the bacterial cell surface

In our previous study, we demonstrated that *G. mellonella* apolipophorin III, a protein involved in the insect immune response, bound to a cell surface of different bacteria [39]. Since it is well known that lysozyme is involved in the antimicrobial activity of insect hemolymph, we tested *G. mellonella* lysozyme binding to a cell surface of different Gram-positive and Gram-negative bacteria. The bacteria were incubated with a *G. mellonella* hemolymph extract (5 μg of total protein) containing lysozyme and the proteins adsorbed on the cell surface were analyzed by SDS-PAGE and, after electrotransfer onto the PVDF membrane, by immunoblotting with anti-*G. mellonella* lysozyme antibodies (Fig. 4). The analysis revealed that *G. mellonella* lysozyme bound to the cell surface of all Gram-positive as well as Gram-negative bacteria tested.

3.3. Permeabilization of the Gram-negative bacteria membrane by G. mellonella lysozyme

The immunoblotting analysis revealed that *G. mellonalle* lysozyme adsorbed not only to the cell surface of the Gram-positive bacteria but also to the cell surface of the Gram-negative ones. This prompted us to investigate its possible role in the fight against Gram-negative bacteria in insects. In these experiments, the level of cell membrane perforation in *E. coli* JM83 was estimated based on the level of activity of β-galactosidase released from the damaged cells (Fig. 5). Prior to β-galactosidase activity measurements, the bacteria were incubated in the presence of lysozyme in the concentrations 0.5 μM and 5.0 μM, reflecting lysozyme concentrations in non-immune and immune hemolymph of *G. mellonella*, respectively [17]. Moreover, the bacteria were incubated with GMAP2 in the concentration 5.0 μM. The effect of GMAP2 on the level of *E. coli* membrane perforation by lysozyme was also studied. As presented in Fig. 5, the bacteria treated with 0.5 μM and 5.0 μM lysozyme exhibited a perforation level of 4.9% and 21.6%, respectively, indicating that *G. mellonella* lysozyme could permeabilize also Gram-negative bacteria membranes. Interestingly, when the bacteria were incubated with 5.0 μM lysozyme and GMAP2, the perforation level was considerably higher (41.3%), whereas GMAP2 alone did not permeabilize *E. coli* cells. Moreover, treatment of the bacteria with a mixture of 5 μM GMAP2 and 0.5 μM lysozyme increased the perforation level almost to that caused by 5.0 μM lysozyme alone (16.3% and 21.6%, respectively), indicating that the concentrations of both compounds in non-immune hemolymph could be high enough to permeabilize and finally effectively kill the bacterial cells (Fig. 5).

It was studied also if the direct formation of an intermolecular complex could explain the observed effect of GMAP2 on lysozyme permeabilizing activity. To elucidate this possibility, the size exclusion chromatography of the preincubated mixtures of both compounds was performed as described in Materials and methods. The obtained results were negative, no additional peak of the complex was observed, while both the heights as well as the retention times of lysozyme and GMAP2 peaks were identical to those ones observed in case of chromatographic separations of individual molecules (data not shown).

3.4. The effect of G. mellonella lysozyme and anionic peptide 2 on the cell surface of Gram-negative bacteria

After incubation in the presence of lysozyme (5.0 μM) and AP2 (5.0 μM), *E. coli* JM83 cells were imaged using AFM, which allowed analyses of the alterations in the bacterial cell surface caused by the compounds studied (Figs. 6, 7). The control and BSA-treated cells were rod-shaped and covered with relatively regular, small granular structures; however, some cells exhibited additional long flat grooves on the surface (Figs. 6, 7). The RMS roughness values for the control and BSA-treated cells were calculated as 26.12 (±12.30) and 34.84 (±12.28), respectively. When the bacteria were incubated in the

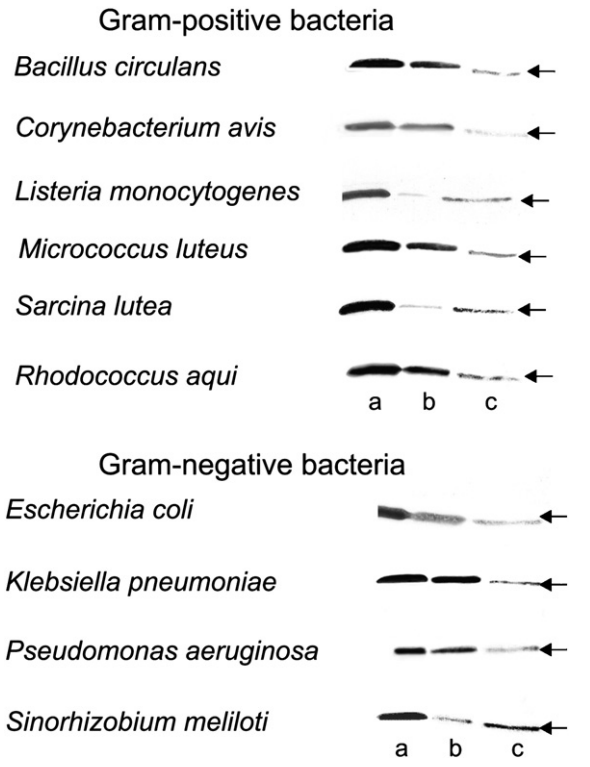

Fig. 4. Binding of *G. mellonella* lysozyme to the bacterial cell surface. The bacteria were incubated with the hemolymph extracts (5 μg of the total protein) as described in Material and methods. The proteins eluted from the bacterial surface (c), present in supernatant (b), and total extract proteins (a, control) were then resolved by Tris-glycine SDS-PAGE, electroblotted onto Immobilon membranes and probed with anti-lysozyme antibodies. Fragments of the membranes presenting lysozyme recognized by the antibodies are demonstrated. Lysozyme that bound to the bacterial cells (c) is additionally marked by the arrows.

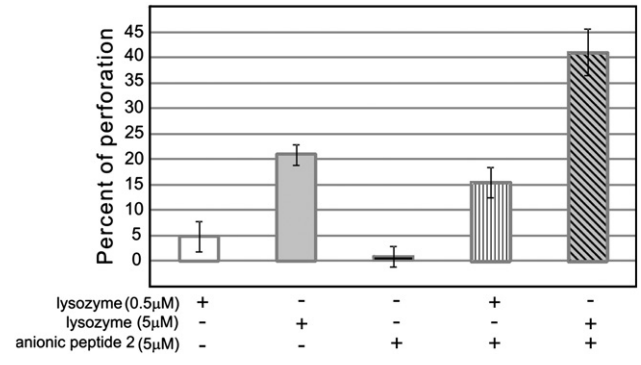

Fig. 5. The effect of *G. mellonella* anionic defense peptide 2 on the level of perforation of *E. coli* cells caused by lysozyme. The bacteria were incubated without or in the presence of lysozyme and GMAP2 as described in Material and methods. Then the β-galactosidase colorimetric substrate was added and the perforation level was determined by measuring absorbance at 405 nm. The perforation level of the dead and live bacteria incubated without any addition was treated as 100% and 0%, respectively. The concentrations of the compounds are given below the diagram. The diagram presents the results ± SD of three independent experiments each performed in triplicate.

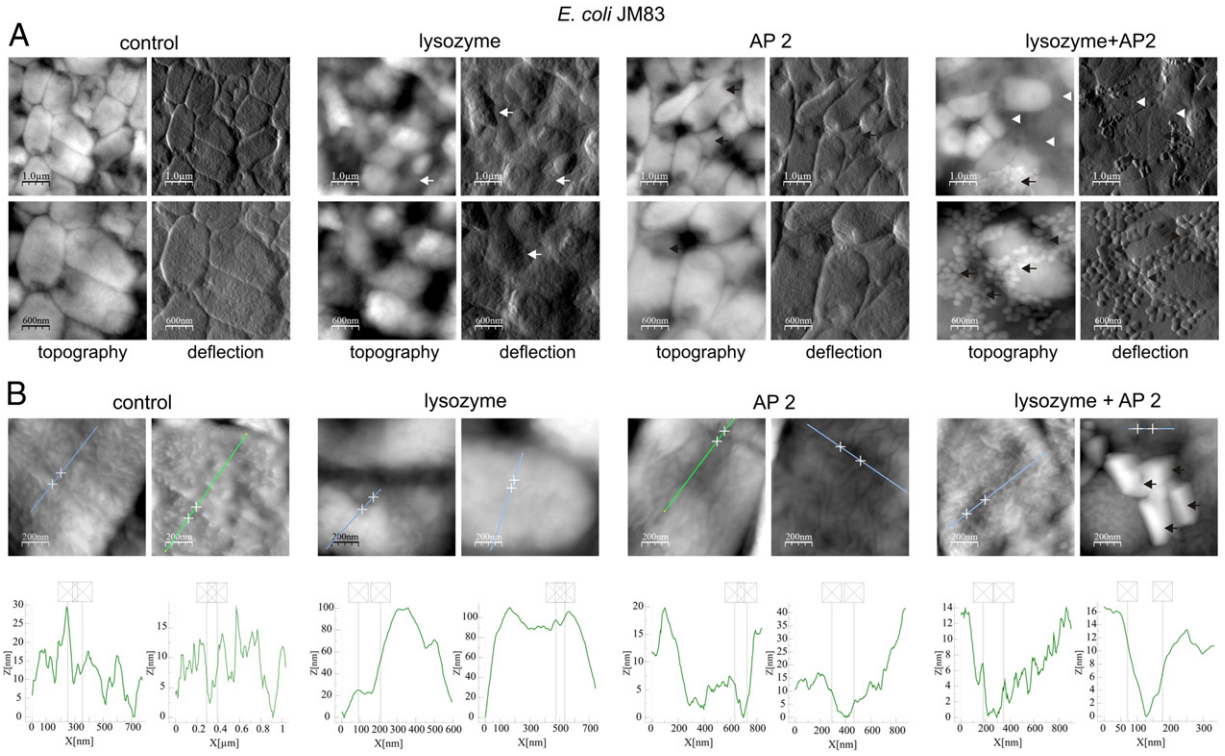

Fig. 6. The effect of *G. mellonella* lysozyme (5.0 μM) and anionic peptide 2 (5.0 μM) on *E. coli* cells. The bacteria were incubated without (control) or in the presence of lysozyme (5.0 μM), anionic peptide 2 (5.0 μM) or the combination of both compounds as described in Materials and methods and then imaged by AFM. (A) Topography and deflection images of the bacterial cells are presented. The white arrows indicate disordered cellular debris of the lysozyme-treated bacteria. The black arrows mark poorly pronounced contours of the GMAP2-exposed cells. The white and black arrowheads indicate damaged cells and regular extracellular crystals, respectively, visible after incubation of bacteria with the combination of lysozyme and GMAP2. (B) Topography images taken from two randomly selected areas on the mica disk (upper panels) and section profiles corresponding to the lines in the images (bottom panels) are presented (magnification 135,000×). The black arrows mark regular extracellular crystals observed after incubation of bacteria with the combination of lysozyme and GMAP2.

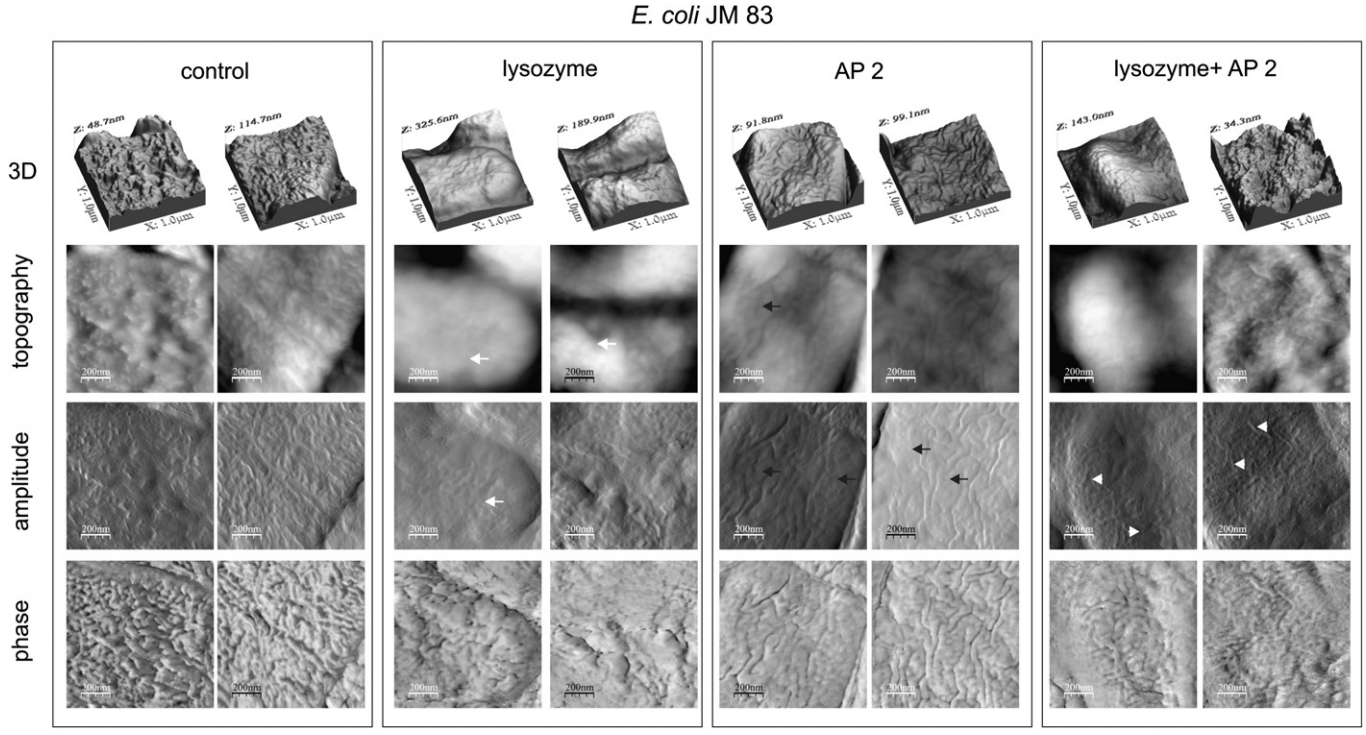

Fig. 7. The alterations in the *E. coli* cell surface caused by *G. mellonella* lysozyme (5.0 μM) and anionic peptide 2 (5.0 μM). The bacteria were incubated without (control) or in the presence of lysozyme (5.0 μM), anionic peptide 2 (5.0 μM) or the combination of both compounds as described in Materials and methods and then imaged by AFM. The 3D, topography, amplitude and phase images of the bacterial cell surface taken from two randomly selected areas on the mica disk are presented (magnification 135,000×). The white arrows indicate grooves on the cell surface of the lysozyme-treated bacteria. The black arrows mark smooth areas between the wrinkles on the cell surface of GMAP2-exposed bacteria. The white arrowheads indicate non-regular grain and furrows on the cell surface of bacteria incubated with both compounds.

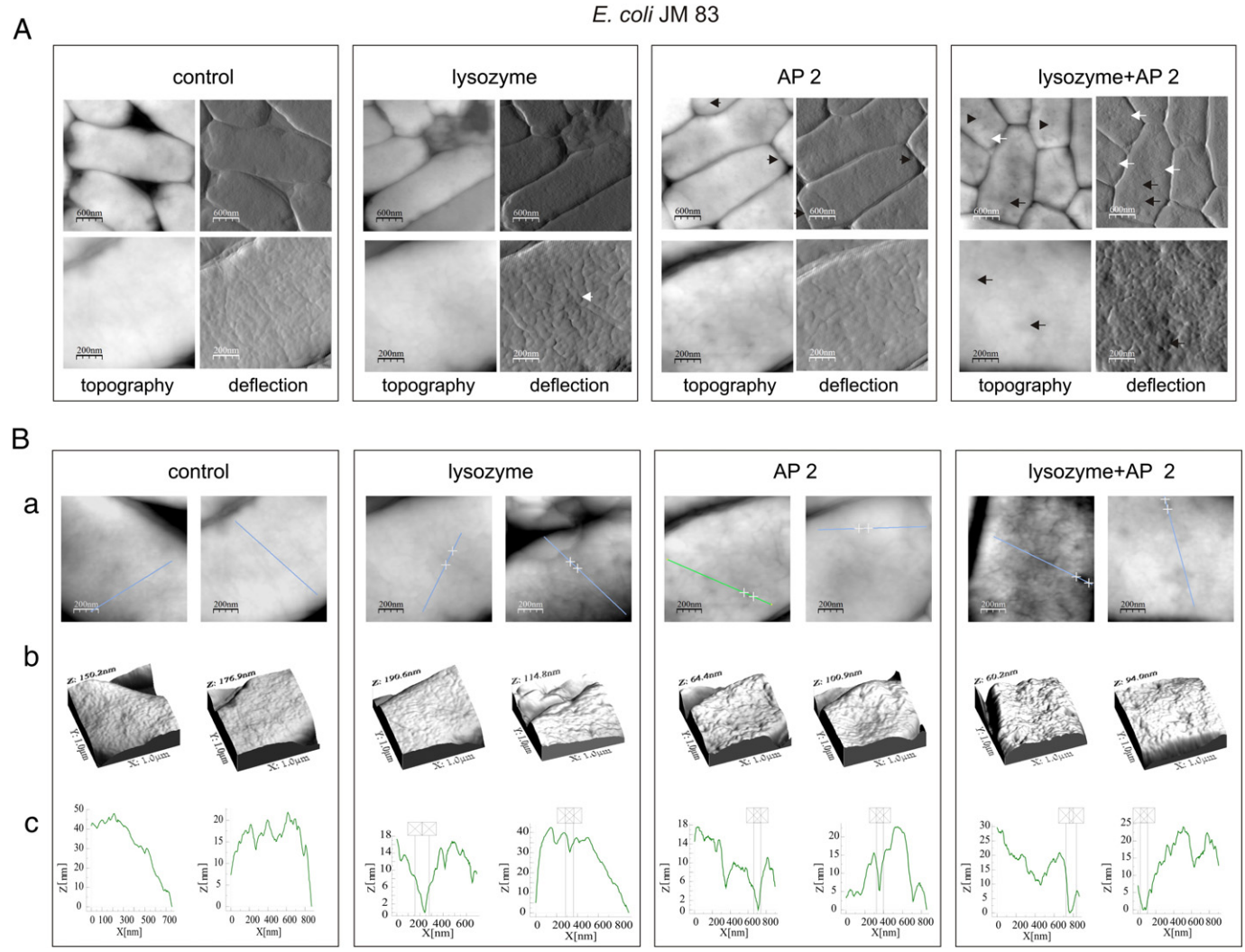

Fig. 8. Analysis of *E. coli* cell surface alterations after incubation with *G. mellonella* lysozyme (1.0 μM) and anionic peptide 2 (1.0 μM). The bacteria were incubated without (control) or in the presence of lysozyme (1.0 μM), anionic peptide 2 (1.0 μM) or the combination of both compounds as described in Materials and methods and then imaged by AFM. (A) Topography and deflection images of the bacterial cells are presented. The white arrows indicate granular structures on the surface of the lysozyme-treated bacteria. The black arrows mark the non-round ends of the GMAP2-exposed cells. The white and black arrowheads indicate the angular ends of cells and surface holes, respectively, visible after incubation of bacteria with the combination of lysozyme and GMAP2. (B) Topography (a) and 3D (b) images taken from two randomly selected areas on the mica disk and section profiles corresponding to the lines in the images (c) are presented (magnification 135,000×).

presence of lysozyme, some cells were damaged and they formed disordered structures with the presence of cell debris (Fig. 6). Moreover, the cell surfaces were also altered in comparison to the control cells. Deep grooves appeared, whereas the small granular structures disappeared from the surface (Fig. 7). Although incubation of the bacteria with GMAP2 did not cause evident changes in the cell shape, it seemed to induce a decrease in the turgor as the contours of the individual cells became less pronounced than those of the control ones (Fig. 6). Moreover, GMAP2 induced cell surface alterations (Fig. 7). The cells were still covered by wrinkles; however, the cell surface regions between the wrinkles were much smoother than in the control cells. The wrinkles were less numerous and shallower (Fig. 7; see the amplitude and phase images). After treatment of *E. coli* with both compounds, many of the cells were disrupted. The non-disrupted cells seemed to be immersed in an amorphous material, probably a content released from or the debris of the disrupted ones (Fig. 6). Instead of the small granular structures, the surface of the non-damaged cells was decorated by non-regular grain and furrows (Fig. 7). The alterations in the bacteria cell surface caused by the compounds studied were also reflected by differences of cell section profiles, as indicated in Fig. 6B. Although well visible, the alterations did not influence much the roughness of *E. coli* cells. The RMS roughness values of lysozyme- and GMAP2-treated cells were calculated as 37.63 (±15.59) and 37.33 (±15.86), respectively, whereas those exposed to both compounds were calculated as 29.76 (±12.09). In contrast, the analysis of the force values revealed changes in elasticity and adhesion properties of the cells after treatment with lysozyme and GMAP2. Young's modulus, reflecting cell elasticity, decreased significantly from 92.67 MPa (±19.12) in the control cells to 78.02 MPa (±7.37; $p = 0.023$) in *E. coli* cells exposed to a mixture of lysozyme and GMAP2. Incubation of *E. coli* in the presence of lysozyme or GMAP2 did not influence considerably the cells' elasticity. Young's modulus values were calculated as 84.08 MPa (±11.08) and 97.5 MPa (±8.05) for lysozyme- and GMAP2-treated cells, respectively. The measurements of adhesion to the AFM tip indicated that lysozyme and GMAP2 altered adhesion properties of *E. coli* cells. The adhesion force of the control cells was calculated as 1.71 nN (±0.34), whereas of those treated with lysozyme and lysozyme-GMAP2 mixture as 3.68 nN (±0.73; $p = 1.23E-06$) and 2.54 nN (±0.58; $p = 0.001$), respectively. GMAP2 alone did not influence considerably adhesion properties of *E. coli* cells which was reflected by adhesion force calculated as 2.12 nN (±0.37; $p = 0.064$). Interestingly, regular extracellular structures were noticed in the AFM images of the bacteria incubated with a mixture of lysozyme and GMAP2. The

structures covered some bacterial cells and were visible between the cells (Fig. 6). To determine the nature of these structures, the samples were imaged using SEM and X-ray analysis was performed (see Subsection 3.5).

Since the *E. coli* cells treated with the above-mentioned concentrations of *G. mellonella* lysozyme and GMAP2 were seriously damaged, a lower concentration (1.0 μM) of the compounds studied was used in the following experiments. This facilitated demonstration of subtle alterations in the bacterial cell shape and surface occurring under the influence of both factors (Fig. 8). The surface of the cells incubated with 1.0 μM lysozyme was more wrinkled than in the control ones and irregular granular structures as well as grooves were detected. The irregularities were well reflected by the profiles presented in Fig. 8B. The RMS roughness values of the control and lysozyme-exposed cells were calculated as 16.60 (±7.77) and 11.13 (±4.44; $p=0.0004$), respectively. GMAP2 (1.0 μM) altered the surface of *E. coli* cells as well, in comparison to the control ones. The granular structures were less regular and the furrows were dipper. The RMS roughness value for the GMAP2-treated cells was calculated as 8.71 (±2.8; $p=0.0002$). Moreover, the cell shape was also affected. Although the cells were still rod-shaped, their tips were less round than in the control ones and they adhered more one to another (Fig. 8). The alterations of *E. coli* cell surface caused by lysozyme and GMAP2 used in combination were more pronounced than the changes caused by the compounds used alone. First of all, the cells were very closely packed one next to another, which led to evident changes in the cell shape (indicated by the arrowheads in Fig. 8A), suggesting a decrease in turgor pressure. Moreover, in addition to irregular small granulations covering the cell surface, 100 nm diameter holes were detected (Fig. 8). The alterations were also reflected by changes in the RMS roughness value, which for these cells was calculated as 11.43 (±4.9; $p=0.001$).

The effect of *G. mellonella* lysozyme (1.0 μM) and AP2 (1.0 μM) on *E. coli* cells was also imaged using scanning electron microscopy (Fig. 9). The overall surface of cells incubated in the presence of lysozyme became corrugated, whereas the tips of cells treated with GMAP2 exhibited an altered structure, in comparison to the control ones. Additionally, small bubble-like structures were noticed on the slightly corrugated surface of the bacteria exposed to both compounds (Fig. 9).

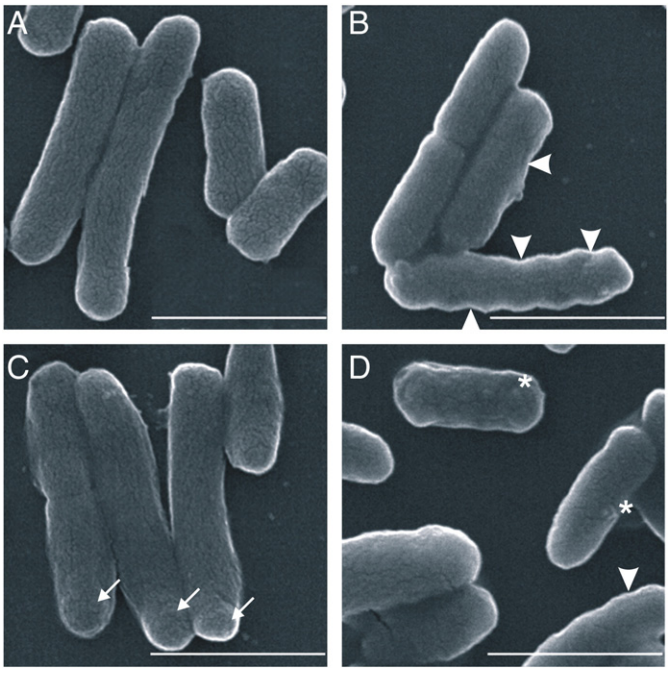

Fig. 9. Scanning electron microscopy images of *E. coli* cells treated with *G. mellonella* lysozyme and anionic peptide 2. The bacteria were incubated without (A; control) or in the presence of lysozyme (B; 1.0 μM), anionic peptide 2 (C; 1.0 μM) or the combination of both compounds (D) as described in Materials and methods and then imaged by SEM. The arrows and arrowheads indicate corrugated cell surface and altered structure of tips, respectively. The asterisks mark bubble-like structures. Single bar = 1 μm (magnification 40,000×).

To test whether the treatment with *G. mellonella* lysozyme and GMAP2 induced the alterations in the cell surface of other Gram-negative bacteria, similar experiments were performed using *K. pneumoniae* (Fig. 10). AFM images revealed that the control cells had characteristic wrinkles resembling cortex bends with some granular structures described previously [43]. Treatment of *K. pneumoniae* cells with lysozyme (1.0 μM) led to disappearance of the cortex bend-like wrinkles. Instead, the cell surface was coated with small, sharp granules (Fig. 10A). In contrast, the wrinkles and grooves were visible on the surface of GMAP2-treated cells (1.0 μM); however, their arrangement and dimensions were different in comparison to the control cells. Moreover, the shape of some cells was altered. The cell surface of *K. pneumoniae* incubated in the presence of both *G. mellonella* lysozyme and GMAP2 underwent considerable alterations, dissimilar to those described above. The cells became smoother, and the granules and wrinkles were shallower. The cell surface seemed to be additionally covered with some amorphous material masking the inequalities noticed on the surface of the cells in the other samples. In addition, evident alterations of the cell shape were observed. The cells were much more convex (*ca.* 80–120 nm height) than those in the other samples (*ca.* 15–40 nm height), probably as a result of swelling (Fig. 10). The *K. pneumoniae* cell surface alterations were well reflected by the changes in the RMS roughness values, which were calculated as 47.11 (±17.61), 25.38 (±15.87; $p=0.0006$), 25.19 (±14.82; $p=0.0003$) and 68.53 (±23.74; $p=0.005$), for the control, lysozyme-GMAP2-treated cells, and cells incubated with both compounds, respectively.

3.5. X-ray analysis of rectangular structures

In order to understand the nature of the rectangular structures visible in the AFM images of cells exposed to *G. mellonella* lysozyme (5.0 μM) and GMAP2 (5.0 μM) X-ray elemental microanalysis under SEM was performed on the raw material without shadowing (Fig. 11). The comparison of the results of the analyses of the bacterial surface (control) and the rectangular structures revealed that they were enriched with sodium and chloride. Both these areas demonstrated the relatively high content of aluminum (Al) and silicon (Si), coming from the mica disk, but the differential analysis of spectra, after subtraction of the content of the elements detected in the control areas, indicated that mean content of sodium and chloride in the rectangular structures was 73.93% and 26.07% (wt.), respectively (Fig. 12). Considering the composition of sodium chloride, it can be calculated that about 17% of sodium formed sodium chloride crystals in the rectangular structures detected in samples of bacteria treated with *G. mellonella* lysozyme and AP2. Hence, the structures contained about 43% of sodium chloride. The rest of sodium ions probably formed salts of amino acids.

4. Discussion

In the present study, we demonstrated that the antimicrobial activity of *G. mellonella* lysozyme against Gram-negative bacteria increased considerably in the presence of anionic defense peptide GMAP2. Using the immunoblotting technique, we showed binding of *G. mellonella* lysozyme to the cell surface of selected Gram-positive and Gram-negative bacteria. Anti-Gram-positive bacteria activity of lysozyme, based on its muramidase enzymatic activity, is well documented [31,44]. In our investigations, *G. mellonella* lysozyme used in the concentration 0.015 μM inhibited growth of the Gram-positive bacteria studied, which was accompanied by serious alterations of the cell surface and damage to the cells, as imaged by AFM. Since lysozyme bound to the Gram-negative bacteria, its activity against *E. coli* and *K. pneumoniae* was investigated by us in more detail. The anti-Gram-negative bacteria activity of *G. mellonella*

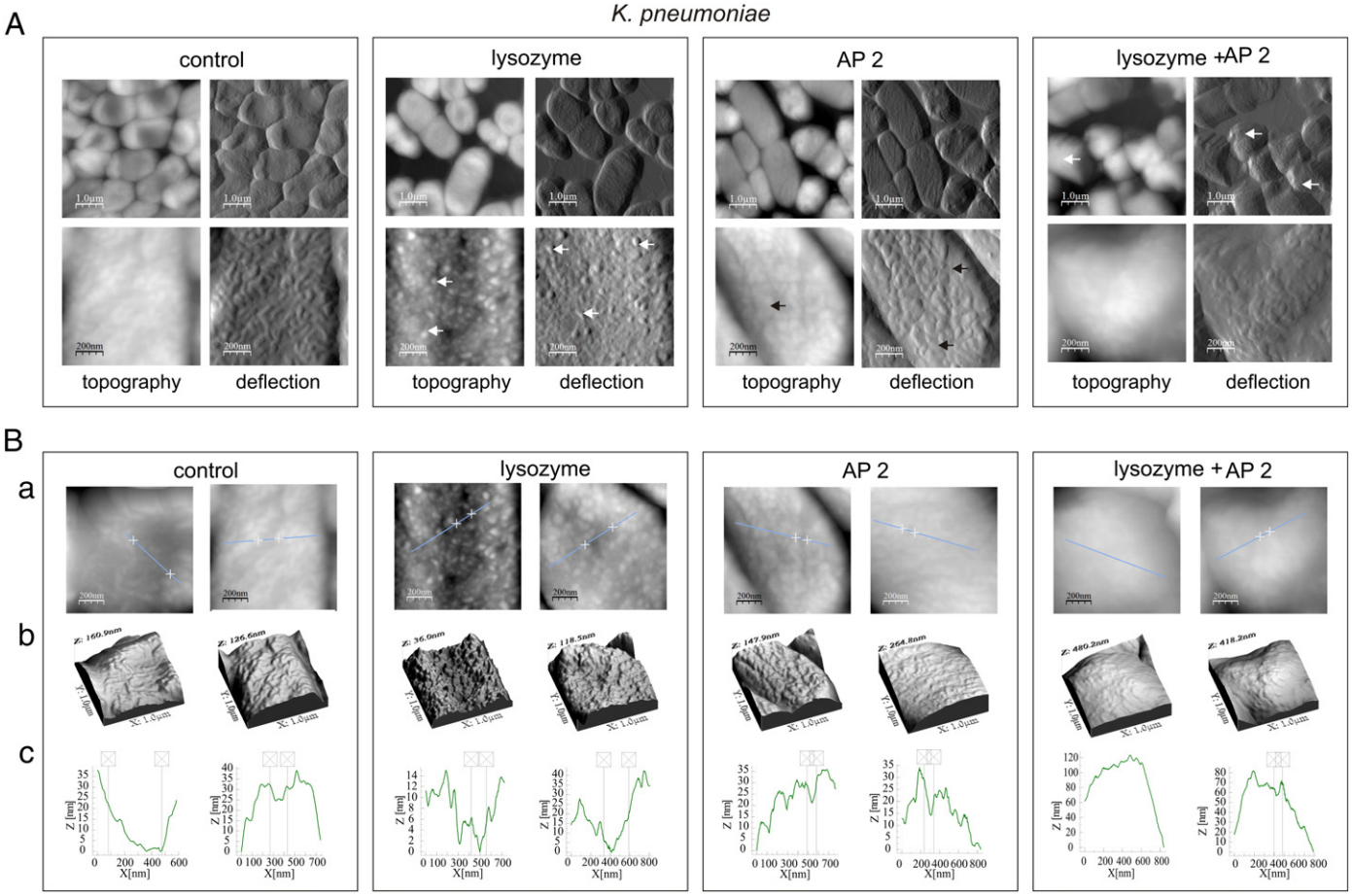

Fig. 10. Analysis of *K. pneumoniae* cell surface alterations after incubation with *G. mellonella* lysozyme (1.0 μM) and anionic peptide 2 (1.0 μM). The bacteria were incubated without (control) or in the presence of lysozyme (1.0 μM), anionic peptide 2 (1.0 μM) or the combination of both compounds as described in Materials and methods and then imaged by AFM. (A) Topography and deflection images of the bacterial cells are presented. The white arrows indicate small, sharp granules on the surface of the lysozyme-treated bacteria. The black arrows mark the altered layout of wrinkles on the surface of the GMAP2-exposed cells. The white arrowheads indicate the cells with a changed shape noticed after incubation of bacteria with the combination of lysozyme and GMAP2. (B) Topography (a) and 3D (b) images taken from two randomly selected areas on the mica disk and section profiles corresponding to the lines in the images (c) are presented (magnification 135,000×).

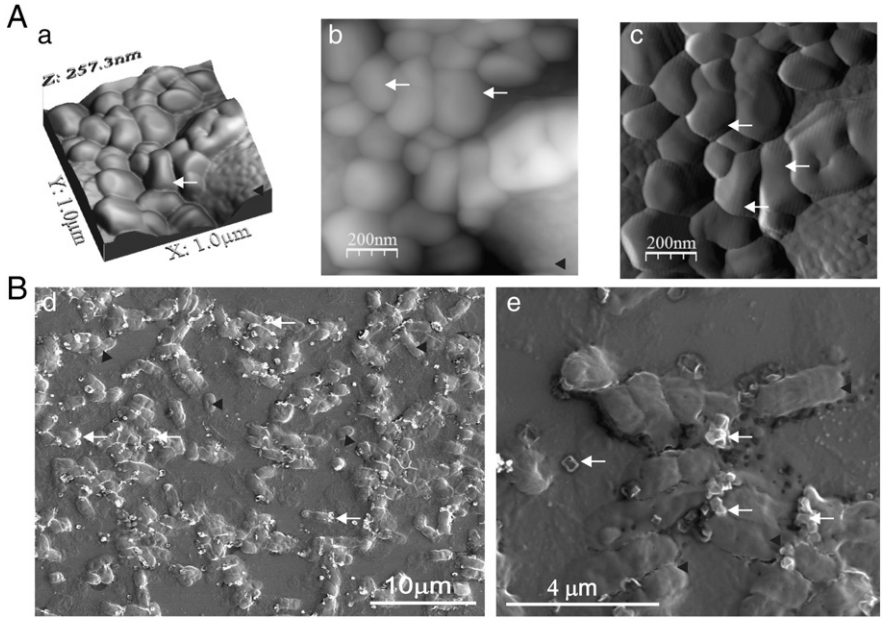

Fig. 11. Microscopic imaging of the extracellular structures appearing after treatment of *E. coli* with the combination of *G. mellonella* lysozyme and anionic peptide 2. The extracellular structures detected in samples of bacteria incubated with lysozyme (5.0 μM) and anionic peptide 2 (5.0 μM) were imaged by AFM (A) and SEM (B). 3D (a), topography (b) and deflection (c) AFM images are presented. Two different magnifications of SEM images, 5000× (d) and 20,000× (e), are demonstrated. The white arrows and the black arrowheads indicate rectangular structures containing sodium chloride and bacterial cells, respectively.

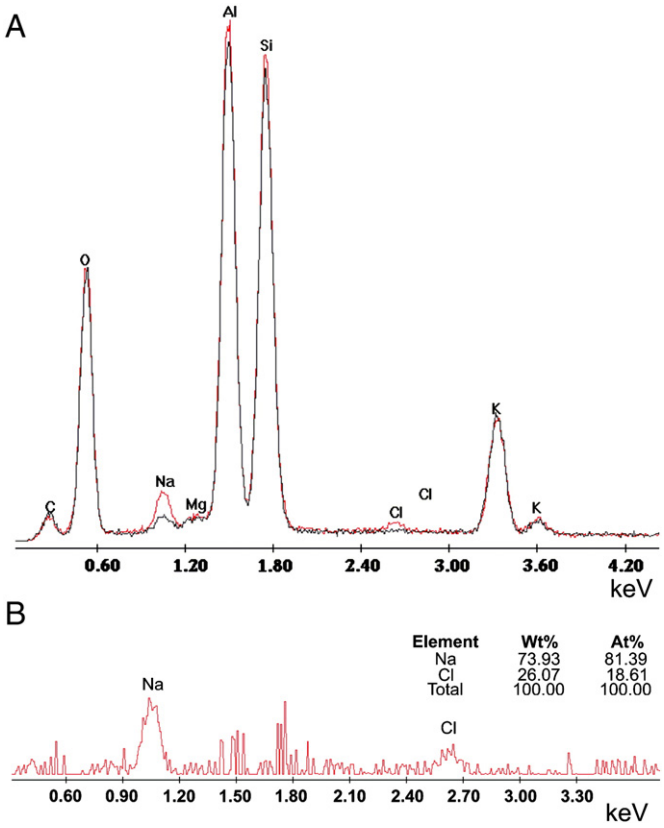

Fig. 12. X-ray microanalysis of the elements of the rectangular structures appearing after treatment of *E. coli* with *G. mellonella* lysozyme and anionic peptide 2. (A) Comparison of the elements content of the rectangular structures (red line) and the control areas (black line). (B) Sodium and chloride content in the rectangular structures – differential analysis of the spectra presented in (A).

lysozyme was reported previously; however, it was relatively low in comparison to the level of the anti-Gram-positive bacteria activity [26]. Two concentrations of lysozyme, 0.5 μM and 5.0 μM, reflecting its concentrations in the hemolymph of naive and bacteria-immunized *G. mellonella* larvae, respectively [17], were used in our experiments. Using a permeabilization assay it was demonstrated that lysozyme in both concentrations could perforate the cell membrane in *E. coli*. Surprisingly, addition of anionic peptide 2 considerably increased the perforation level caused in *E. coli* by 0.5 μM lysozyme to almost that detected for 5.0 μM lysozyme. This result is very meaningful, when one takes into consideration the fact that both lysozyme and GMAP2 are present in the hemolymph of naive *G. mellonella* larvae [17]. The combination of both compounds in the concentrations reflecting those in non-immune hemolymph caused a considerable increase in the perforation level of Gram-negative bacteria, indicating that they could be high enough to kill invading bacterial cells effectively. Hence, thanks to constitutively synthesized factors present in hemolymph, naive *G. mellonella* larvae are to some extent protected against infection caused by Gram-negative bacteria. Our results clearly suggested a synergistic action of lysozyme and GMAP2 in fighting against pathogens. So far, literature data have indicated only a possibility of a synergistic action of lysozyme and cationic insect defense peptides, *e.g.* cecropins, insect defensins and attacins, against *E. coli* [35,36]. A synergistic action of lysozyme and *G. mellonella* defense peptides against *E. coli* as well as lysozyme and *G. mellonella* apoLp-III against Gram-positive *M. luteus* was also suggested [33,34]. Similarly, cationic human defensins HD-1, 2 and 3 as well as bactericidal peptides from hemoglobin (hemocidins) acted synergistically with lysozyme [41,45]. It was also reported that lysozyme decreased MIC for cationic peptide LL-37/hCAP-18 against *Enterococcus faecalis* [46]. However, when anionic peptides of airway surface liquid were tested in the presence of egg white lysozyme or human neutrophil lysozyme, no significant increase in the antimicrobial activity against Gram-positive and Gram-negative bacteria was observed at physiological concentrations [47].

Having discovered that *G. mellonella* GMAP2 and lysozyme could act in concert against Gram-negative bacteria, we were interested in the mechanism of their antimicrobial action. A possibility of intermolecular complex formation between lysozyme and the peptide before their interaction with bacterial membrane was excluded during gel filtration experiment. However, it is generally assumed that the antimicrobial peptides existing as disordered structures in aqueous solutions adopt their proper conformation after exposing to the lipid membrane. The two main conformations induced upon membrane binding are α-helix and β-sheet [5,48–51]. Hence, it cannot be excluded that the contact with bacterial membrane triggers adopting of a proper conformation of GMAP2 or eventually modifies its structure, which allows it to interact with lysozyme, resulting in increase of lysozyme antibacterial activity. However, such possibility is speculative at this moment and requires further studies.

To provide more insight into antimicrobial action of the studied defense factors, the bacteria incubated in the presence of both compounds were imaged using AFM and SEM. The analysis of the images suggested that treatment of the cells with GMAP2 and lysozyme decreased the cell turgor pressure, as the cells became closely packed and lost their proper shape. The analysis of the force values confirmed this hypothesis. Young's modulus of the cells exposed to a mixture of lysozyme and GMAP2 decreased significantly, whereas at the same time adhesive force between the AFM tip and cell surface considerably increased. The detected changes in both parameters reflected a decrease in cell wall elasticity, indicating a decrease in cell turgor pressure.

An exposure of the cells to higher concentrations of lysozyme and GMAP2 (5.0 μM) resulted in appearance of the rectangular structures

containing sodium chloride crystals. These effects could be connected with destabilization of the osmotic balance affecting the cell volume. In proper regulation of the cell volume and osmotic balance, the ion channels (sodium, potassium, calcium, and chloride) and integral membrane proteins allowing movement of ions across the membrane down their electrochemical gradients are involved. In bacterial cell membranes, different ion channels and substrate transporting systems have been described. Especially, various sodium–substrate co-transport systems deliver *e.g.* amino acids, melibiose, and glutamate into the bacterial cell. A gradient of sodium ions provides energy for entry of the substrate against the concentration gradient [52–54]. It is possible that crystallization of sodium chloride occurred during preparation of samples for AFM imaging. However, appearance of the sodium chloride crystals after treatment of *E. coli* cells with *G. mellonella* lysozyme and GMAP2 suggested that these compounds used in combination could cause electrolyte imbalance and cell dehydration leading to a decrease in the cell turgor pressure and, finally, to disruption of the cells.

It is worth to emphasize that the above-mentioned effects were not noticed when lysozyme and GMAP2 were used alone against *E. coli*. Moreover, GMAP2 did not perforate *E. coli* cells at all, even at the concentration of 5.0 μM, suggesting that the peptide increased the antibacterial activity of lysozyme. Interestingly, GMAP2 did not influence the level of *G.mellonella* lysozyme muramidase activity in our assay using *M. luteus* lyophilized cells (data not shown). Although GMAP2 did not increase the muramidase activity, it could alter the *E. coli* cell surface characteristics facilitating lysozyme binding and access to the peptidoglycan layer. However, it is known that apart from muramidase, the antibacterial properties of lysozyme can be attributed to its non-enzymatic activity, related to the cationic properties of the protein molecule or to its particular cationic peptide fragments [55,56]. From this point of view, the influence of GMAP2 on this mode of lysozyme action cannot be excluded and requires further biochemical investigation.

Acknowledgements

The authors wish to thank to Prof. Teresa Jakubowicz for her helpful remarks concerning the conducted studies and the present paper. The work was financially supported by grant N N303 362235 from the Polish Ministry of Science and Higher Education. The Faculty of Biochemistry, Biophysics, and Biotechnology of the Jagiellonian University is a beneficiary of the structural funds from the European Union (Grant No. POIG.02.01.00-12-064/08 “Molecular Biotechnology for Health”).

References

[1] P. Bulet, R. Stöcklin, L. Menin, Anti-microbial peptides: from invertebrates to vertebrates, Immunol. Rev. 198 (2004) 169–184.
[2] H. Jenssen, P. Hamil, R.E.W. Hancock, Peptide antimicrobial agents, Clin. Microbiol. Rev. 19 (2006) 491–511.
[3] J.D.F. Hale, R.E.W. Hancock, Alternative mechanisms of action of cationic antimicrobial peptides on bacteria, Expert Rev. Anti Infect. Ther. 5 (2007) 951–959.
[4] R.E.W. Hancock, K.L. Brown, N. Mookherjee, Host defence peptides from invertebrates — emerging antimicrobial strategies, Immunobiology 211 (2006) 315–322.
[5] Y. Shai, Mechanisms of the binding, insertion and destabilization of phospholipids bilayer membranes by α-helical antimicrobial and cell non-selective membrane-lytic peptides, Biochim. Biophys. Acta 1462 (1999) 55–70.
[6] T. Theis, U. Stahl, Antifungal proteins: targets, mechanisms and prospective applications, Cell. Mol. Life Sci. 61 (2004) 437–455.
[7] M.R. Yeaman, N.Y. Yount, Mechanisms of antimicrobial peptide action and resistance, Pharmacol. Rev. 55 (2003) 27–55.
[8] L.T. Nguyen, E.F. Haney, H.J. Vogel, The expanding scope of antimicrobial peptide structures and their modes of action, Trends Biotechnol. 29 (2011) 464–472.
[9] W.C. Wimley, K. Hristova, Antimicrobial peptides: successes, challenges and unanswered questions, J. Membr. Biol. 239 (2011) 27–34.
[10] M. Scocchi, A. Tossi, R. Gennaro, Proline-rich antimicrobial peptides: converging to a non-lytic mechanism of action, Cell. Mol. Life Sci. 68 (2011) 2317–2330.
[11] K.A. Brogden, A.J. De Lucca, J. Bland, S. Elliott, Isolation of an ovine pulmonary surfactant-associated anionic peptide bactericidal for *Pasteurella haemolytica*, Proc. Natl. Acad. Sci. U. S. A. 93 (1996) 412–416.
[12] K.A. Brogden, M. Ackermann, P.B. McCray Jr., B.F. Tack, Antimicrobial peptides in animals and their role in host defences, Int. J. Antimicrob. Agents 22 (2003) 465–478.
[13] N. Sitaram, Antimicrobial peptides with unusual amino acid compositions and unusual structures, Curr. Med. Chem. 13 (2006) 679–696.
[14] R. Lai, L.O. Lomas, J. Jonczy, P.C. Turner, H.H. Rees, Two novel non-cationic defensin-like antimicrobial peptides from haemolymph of the female tick, *Amblyomma hebraeum*, Biochem. J. 379 (2004) 681–685.
[15] H. Wen, X. Lan, T. Cheng, N. He, K. Shiomi, Z. Kajiura, Z. Zhou, Q. Xia, Z. Xiang, M. Nakagaki, Sequence structure and expression pattern of a novel anionic defensin-like gene from silkworm (*Bombyx mori*), Mol. Biol. Rep. 36 (2009) 711–716.
[16] M. Cytryńska, P. Mak, A. Zdybicka-Barabas, P. Suder, T. Jakubowicz, Purification and characterization of eight peptides from *Galleria mellonella* immune hemolymph, Peptides 28 (2007) 533–546.
[17] P. Mak, A. Zdybicka-Barabas, M. Cytryńska, A different repertoire of *Galleria mellonella* antimicrobial peptides in larvae challenged with bacteria and fungi, Dev. Comp. Immunol. 34 (2010) 1129–1136.
[18] W. Mohring, B. Messner, Lysozyme as antibacterial agent in honey and bees venom, Acta Biol. Med. Ger. 21 (1968) 85–95.
[19] R.F. Powning, W.J. Davidson, Studies on insect bacteriolytic enzymes-II. Some physical and enzymatic properties of lysozyme from haemolymph of *Galleria mellonella*, Comp. Biochem. Physiol. B 55 (1976) 221–228.
[20] D. Hultmark, H. Steiner, T. Rasmuson, H.G. Boman, Insect immunity. Purification ad properties of three inducible bactericidal proteins from hemolymph of immunized pupae of *Hyalophora cecropia*, Eur. J. Biochem. 106 (1980) 7–16.
[21] P.A. Rossignol, A.M. Lueders, Bacteriolytic factor in the salivary glands of *Aedes aegypti*, Comp. Biochem. Physiol. B 83 (1986) 819–822.
[22] A.G. Spies, J.E. Karlinsey, K.D. Spence, Antibacterial hemolymph proteins of *Manduca sexta*, Comp. Biochem. Physiol. B 83 (1986) 125–133.
[23] I. Morishima, T. Horiba, Y. Yamano, Lysozyme activity in immunized and non-immunized hemolymph during the development of the silkworm, *Bombyx mori*, Comp. Biochem. Physiol. A 108 (1994) 311–314.
[24] Y. Ito, M. Nakamura, T. Hotani, T. Imoto, Insect lysozyme from mouse fly (*Musca domestica*) larvae: possible digestive function based on sequence and enzymatic properties, J. Biochem. (Tokyo) 118 (1995) 546–551.
[25] T.D. Lockey, D.D. Ourth, Purification and characterization of lysozyme from hemolymph of *Heliothis virescens* larvae, Biochem. Biophys. Res. Commun. 220 (1996) 502–508.
[26] K.H. Yu, K. Kim, J. Lee, H. Lee, S. Kim, K. Cho, M. Nam, I. Lee, Comparative study on characteristics of lysozymes from the hemolymph of three lepidopteran larvae, *Galleria mellonella*, *Bombyx mori*, *Agrius convolvuli*, Dev. Comp. Immunol. 26 (2002) 707–713.
[27] B. Altincicek, E. Knorr, A. Vilcinskas, Beetle immunity: identification of immune-inducible genes from the model insect *Tribolium castaneum*, Dev. Comp. Immunol. 32 (2008) 585–595.
[28] M. Chapelle, P.-A. Girard, F. Cousserans, N.-A. Volkoff, B. Duvic, Lysozymes and lysozyme-like proteins from the fall armyworm, *Spodoptera frugiperda*, Mol. Immunol. 47 (2009) 261–269.
[29] H. Vogel, B. Altincicek, G. Glöckner, A. Vilcinskas, A comprehensive transcriptome and immune-gene repertoire of the lepidopteran model host *Galleria mellonella*, BMC Genomics 12 (2011) 308.
[30] R. Regel, S.R. Matioli, W.R. Terra, Molecular adaptation of *Drosophila melanogaster* lysozymes to a digestive function, Insect Biochem. Mol. Biol. 28 (1998) 309–319.
[31] D. Hultmark, Insect lysozymes, in: P. Jollès (Ed.), Lysozymes: Model enzymes in biochemistry and biology, Birkhäuser Verlag, Basel, Switzerland, 1996, pp. 87–102.
[32] A. Vilcinskas, V. Matha, Antimycotic activity of lysozyme and its contribution to antifungal humoral defence reactions in *Galleria mellonella*, Anim. Biol. 6 (1997) 19–29.
[33] M. Cytryńska, A. Zdybicka-Barabas, P. Jabłoński, T. Jakubowicz, Detection of antibacterial polypeptide activity in situ after sodium dodecyl sulfate-polyacrylamide gel electrophoresis, Anal. Biochem. 299 (2001) 274–276.
[34] A.E. Halwani, G.B. Dunphy, Apolipophorin III in *Galleria mellonella* potentiates hemolymph lytic activity, Dev. Comp. Immunol. 23 (1999) 563–570.
[35] P. Engström, A. Carlsson, A. Engström, Z.J. Tao, H. Bennich, The antibacterial effect of attacins from silk moth *Hyalophora cecropia* is directed against the outer membrane of *Escherichia coli*, EMBO J. 3 (1984) 3347–3351.
[36] R. Chalk, H. Townson, S. Natori, H. Desmond, P.J. Ham, Purification of an insect defensin from the mosquito, *Aedes aegypti*, Insect Biochem. Mol. Biol. 24 (1994) 403–410.
[37] M. Cytryńska, A. Zdybicka-Barabas, T. Jakubowicz, Studies on the role of protein kinase A in humoral immune response of *Galleria mellonella* larvae, J. Insect Physiol. 52 (2006) 744–753.
[38] H. Schägger, G. von Jagow, Tricine–sodium dodecyl sulfate-polyacrylamide gel electrophoresis for the separation of proteins in the range from 1 to 100 kDa, Anal. Biochem. 166 (1987) 368–379.
[39] A. Zdybicka-Barabas, M. Cytryńska, Involvement of apolipophorin III in antibacterial defense of *Galleria mellonella* larvae, Comp. Biochem. Physiol. B 158 (2011) 90–98.
[40] U.K. Laemmli, Cleavage of structural proteins during the assembly of the head of bacteriophage T4, Nature 277 (1970) 680–685.
[41] P. Mak, M. Siwek, J. Pohl, A. Dubin, Menstrual hemocidin HbB115-146 is an acidiphilic antibacterial peptide potentiating the activity of human defensins, cathelicidin and lysozyme, Am. J. Reprod. Immunol. 57 (2007) 81–91.
[42] M.M. Bradford, A rapid and sensitive method for the quantitation of microgram quantities of protein utilizing the principle of protein-dye binding, Anal. Biochem. 72 (1976) 248–254.
[43] A. Zdybicka-Barabas, B. Januszanis, P. Mak, M. Cytryńska, An atomic force microscopy study of *Galleria mellonella* apolipophorin III effect on bacteria, Biochim. Biophys. Acta 1808 (2011) 1896–1906.

[44] B. Masschalck, C.W. Michiels, Antimicrobial properties of lysozyme in relation to foodborne vegetative bacteria, Crit. Rev. Microbiol. 29 (2003) 191–214.
[45] D. Schnapp, A. Harris, Antibacterial peptides in bronchoalveolar lavage fluid, Am. J. Respir. Cell Mol. Biol. 19 (1998) 352–356.
[46] R. Bals, X.R. Wang, M. Zasloff, J.M. Wilson, The peptide antibiotic LL-37/hCAP-18 is expressed in epithelia of the human lung where it has broad antimicrobial activity at the airway surface, Proc. Natl. Acad. Sci. U. S. A. 95 (1998) 9541–9546.
[47] V.C. Kalfa, K.A. Brogden, Anionic antimicrobial peptide-lysozyme interactions in innate pulmonary immunity, Int. J. Antimicrob. Agents 13 (1999) 47–51.
[48] S.E. Blondelle, K. Lohner, M.-I. Aguilar, Lipid-induced conformation and lipid-binding properties of cytolytic and antimicrobial peptides: determination and biological specificity, Biochim. Biophys. Acta 1462 (1999) 89–108.
[49] H. Sato, J.B. Feix, Peptide-membrane interactions and mechanisms of membrane destruction by amphipathic α-helical antimicrobial peptides, Biochim. Biophys. Acta 1758 (2006) 1245–1256.
[50] M. Mihajlovic, T. Lazaridis, Atimicrobial peptides in toroidal and cylindrical pores, Biochim. Biophys. Acta 1798 (2010) 1485–1493.
[51] N. Sitaram, R. Nagaraj, Interaction of antimicrobial peptides with biological and model membranes: structural and charge requirements for activity, Biochim. Biophys. Acta 1462 (1999) 29–54.
[52] P. Koprowski, A. Kubalski, Bacterial ion channels and their eukaryotic homologues, Bioessays 23 (2001) 1148–1158.
[53] M. Roeßler, V. Müller, Osmoadaptation in bacteria and archaea: common principles and differences, Environ. Microbiol. 3 (2001) 743–754.
[54] T.H. Wilson, P.Z. Ding, Sodium–substrate cotransport in bacteria, Biochim. Biophys. Acta 1505 (2001) 121–130.
[55] A. Pellegrini, U. Thomas, N. Bramaz, S. Klauser, P. Hunziker, R. von Fellenberg, Identification and isolation of a bactericidal domain in chicken egg white lysozyme, J. Appl. Microbiol. 82 (1997) 372–387.
[56] K. Düring, P. Porsch, A. Mahn, O. Brinkmann, W. Gieffers, The non-enzymatic microbicidal activity of lysozymes, FEBS Lett. 449 (1999) 93–100.